Yonago Acta Medica 2023;66(1):78–86 doi: 10.33160/yam.2023.02.009 *Original Article*

Imaging of Liver Tissues Using a Combination of Silver Impregnation and Low-Vacuum Scanning Electron Microscopy; A Simple Method for the High-Resolution Visualization of Reticulin Structures with Applicability to a Quantitative Analysis

Mikihiro Izuta,*‖ Satoshi Kuwamoto,† Tetsutaro Kamiya,* Keiko Nagata,‡ Michiko Matsushita,* Sumire Inaga,§ Toshiyuki Kaido,§ Yoshihisa Umekita,† Kazuhiko Hayashi† and Yukisato Kitamura*

**Department of Pathobiological Science and Technology, School of Health Science, Faculty of Medicine, Tottori University, Yonago 683-8503 Japan, †Department of Pathology, School of Medicine, Faculty of Medicine, Tottori University, Yonago 683-8503 Japan, ‡Division of Pharmacology, Department of Pathophysiological and Therapeutic Sciences, School of Medicine, Faculty of Medicine, Tottori University, Yonago 683-8503 Japan, §Department of Anatomy, School of Medicine, Faculty of Medicine, Tottori University, Yonago 683-0853, Japan*

ABSTRACT

Background Low-vacuum scanning electron microscopy (LVSEM) enables the detailed three-dimensional imaging of archival tissues without special pretreatments. The clinical utility of LVSEM in the assessment of liver diseases has not yet been defined. So, we investigated the utility of LVSEM imaging in morphological assessments of normal and diseased liver tissues, with a focus on reticulin structures.

Methods Formalin-fixed tissue samples of two normal livers and two hepatocellular carcinomas with background regenerative nodules/areas were stained with platinum blue stain or silver-impregnated using Watanabe's method and then comparatively observed under LVSEM. We also evaluated the applicability of LVSEM imaging of liver tissues to a quantitative analysis using a digital image analysis technique.

Results Optimal high-resolution images of reticulin structures were obtained using 10-μm-thick silver-impregnated sections. Reticulin fibers were clearly observed to run dendritically around sinusoids in normal livers, and markedly increased in regenerative nodules/areas. Normal reticulin frameworks were lost in hepatocellular carcinoma, leaving a few fragments of reticulin fibers within tumors. Moreover, when a quantitative analysis was applied to these images, we successfully demonstrated a significantly higher reticulin fiber density in regenerative nodules/areas than in the normal liver ($P < 0.05$).

Conclusion We not only obtained detailed three-dimensional images of reticulin structures in various liver tissues by LVSEM combined with silver impregnation but also showed their applicability to a quantitative analysis. The method presented herein may be applied to future studies for the more accurate diagnosis and better classification/risk stratification of various liver diseases.

Key words carcinoma, hepatocellular; liver diseases; microscopy, electron, scanning; image processing, computer-assisted; reticulin

Reticulin fibers are major components of the extracellular matrix and are mainly composed of type III collagen.[1] In the normal liver, they form a fine reticular framework that lines hepatocyte plates, serving as a scaffold for hepatocytes.[2] Although these fibers are not stained with conventional hematoxylin and eosin (HE), they stain darkly with a silver impregnation method and, thus, are also called argyrophilic fibers.[1] The staining of reticulin fibers is commonly utilized to assess the architecture of hepatocyte plates, in which they are compressed in nodular regenerative hyperplasia and collapsed in necrosis.[3] These fibers are generally lost or decreased in hepatocellular carcinoma (HCC), resulting in areas and/or thickened trabeculae composed of hepatocytes that do not touch reticulin fibers at any of their borders, and this feature has long been used to differentiate HCC from benign hepatocellular lesions.[4] However, alterations in reticulin fibers in liver diseases are typically evaluated by light microscopy (LM) only, and their detailed three-dimensional structures have not yet been adequately examined. Moreover, while collagen fibers in liver fibrosis are routinely assessed by semi-quantitative methods and their exact quantification

‖Present address: Department of Pathology, Kansai Medical University Medical Center, Moriguchi 570-8507, Japan
Mikihiro Izuta and Satoshi Kuwamoto contributed equally to this study.
Corresponding author: Satoshi Kuwamoto, MD, PhD
s.quamoto@gmail.com
Received 2022 October 3
Accepted 2022 December 21
Online published 2023 February 4
Abbreviations: BDL, bile duct ligation; HCC, hepatocellular carcinoma; HE, hematoxylin and eosin; LM, light microscopy; LVSEM, Low-vacuum scanning electron microscopy; Pt-Blue, platinum blue; SEM, scanning electron microscopy; TAA, thioacetamide

Table 1. Summary of subjects

Case No.		1	2	3	4
Age		90	71	64	18
Sex		F	M	M	F
Cause of death		Brain infarction	Myelodysplastic syndrome, lobar pneumonia	HCC	HCC
Liver findings		None	None	Moderately differentiated HCC and cirrhosis	Moderately and well-differentiated HCC, cholestasis, and congestive liver
Probable cause of liver disease		None	None	Excessive alcohol use	Administration of cyproterone acetate
Serum HBsAg		Negative	Not tested	Negative	Negative
Serum HCVAb		Negative	Not tested	Negative	Negative
Laboratory data at the terminal phase	AST (U/L)	75	1278	47	4110
	ALT (U/L)	61	783	23	578
	ALP (U/L)*	657	236	594	1498
	GGT (U/L)	73	15	86	234
	LDH (U/L)	322	763	225	7435
	T-bil (mg/dL)	0.3	1.2	25.6	11.4
	D-bil (mg/dL)	0.1	0.7	17.9	7.9

*According to the Japan Society of Clinical Chemistry-based reference method. ALP, alkaline phosphatase; ALT, alanine aminotransferase; AST, aspartate aminotransferase; D-bil, direct bilirubin; F, female; GGT, gamma-glutamyltranspeptidase; HBsAg, hepatitis B virus surface antigen; HCC, hepatocellular carcinoma; HCVAb, hepatitis C virus antibody; LDH, lactate dehydrogenase; M, male; T-bil, total bilirubin.

has also been actively investigated,[5] few studies have focused on the quantification of reticulin fibers in liver diseases.[2] In consideration of the recent concept that liver fibrosis is reversible when the insult is removed,[6] it may be meaningful to establish a novel method that visualizes reticulin structures in liver diseases in detail and is also applicable to a quantitative analysis.

Low-vacuum scanning electron microscopy (LVSEM) is a recently developed technique that has the advantage of using a lower vacuum than ordinary scanning electron microscopy (SEM). Under a low vacuum, a sample may not only be prevented from drying out, but also the incident electrons or electrons emitted from the sample collide with residual gas molecules to generate cations, which neutralize the electrons that accumulate on the sample, thereby reducing the charge-up phenomenon.[7] This enables non-conductive samples, such as formalin-fixed archival tissues, to be directly subjected to LVSEM observations without metal coatings and their detailed three-dimensional structure to be visualized.[8]

In the present study, we investigated the potential utility of LVSEM for a detailed evaluation of morphological alterations in liver diseases, with a focus on reticulin structures. We examined two cases of HCC with background regenerative nodules or regenerative areas. Two normal livers were also investigated as controls. After selecting the optimal sample thickness for LVSEM observations, samples were stained with platinum blue (Pt-Blue) or silver-impregnated using Watanabe's method and then comparatively observed under LVSEM. In comparisons with the Pt-Blue stain, which has been used as the standard electron staining technique for LVSEM,[8–10] silver impregnation highlighted reticulin fibers more clearly, enabling easier observations of their three-dimensional structures in both normal and diseased liver tissues. To the best of our knowledge, this is the first study to apply the combination of silver impregnation and LVSEM to the detailed visualization of reticulin structures in the liver. We also investigated whether this novel method may be applied to a quantitative analysis of reticulin fibers.

MATERIALS AND METHODS

Materials

We prepared formalin-fixed paraffin-embedded liver

tissues from two autopsy cases with no known liver diseases (Case Nos. 1 and 2) and two of HCC (Case Nos. 3 and 4). Patient profiles and laboratory data at the terminal phase are shown in Table 1. Samples from case Nos. 1 and 2 were regarded as almost normal based on conventional light microscopic observations and used as normal controls. Although both cases showed elevated liver enzymes to varying degrees, these changes were considered to be caused by ischemic hepatitis (so-called shock liver) at the terminal phase and only had a minimal effect on liver histology, except for mild centrilobular congestion. HCC cases had coexisting liver cirrhosis (Case No. 3) or liver cholestasis/congestion (Case No. 4) and, thus, regenerative nodules or regenerative areas were present in background liver tissues. Excessive alcohol use in case No. 3 and the long-term administration of cyproterone acetate for precocious puberty in case No. 4 were considered to be the causes of their liver diseases.

The present study was approved by the Ethics Review Committee of Tottori University, Faculty of Medicine (No.19A197).

Selection of the optimal sample thickness for LVSEM observations

To select the optimal thickness for LVSEM observations with each stain, we prepared 5-, 10-, and 20-μm-thick sections of a normal liver (Case No. 1) and subjected them to Pt-Blue staining or silver impregnation (Watanabe's method). We selected 5 and 10 μm as the optimal thicknesses for Pt-Blue staining and silver impregnation, respectively (see Results), which were applied to subsequent analyses.

Staining

After selecting optimal sample thicknesses, 5- and 10-μm-thick sections of Case Nos. 2–4 were prepared and subjected to Pt-Blue staining and silver impregnation, respectively. We selected these staining methods because Pt-Blue is currently the standard method for LVSEM[8–10] and silver impregnation is commonly used to visualize reticulin fibers, taking advantage of their argyrophilic property. We also performed HE staining on each specimen for a conventional morphological analysis.

Observations

HE- and Pt-Blue-stained sections were observed by LM and LVSEM (Miniscope TM-3030Plus, Hitachi High-Tech Corporation, Tokyo, Japan), respectively, and silver-impregnated sections by LM and LVSEM. Images were obtained using either the backscattered electron (BSE), secondary electron (SE), or mixed (BSE + SE) observation mode at room temperature with an acceleration voltage of 15 kV and vacuum of 50 Pa.

Quantification of reticulin fiber density

LVSEM images of silver-impregnated liver sections (Case Nos. 1–4) captured at ×1,000 magnification (8 bit, grayscale) were subjected to a quantitative analysis of reticulin fiber density. Using ImageJ,[11] we extracted areas of reticulin fibers by manually thresholding the gray value, producing binary images that only displayed the areas of reticulin fibers. By using the "Rectangle" tool and ROI manager, at least 5 regions that were appropriate for the quantitative analysis (regions at which reticulin fibers were distributed parallel to the image plane) were selected, and the mean gray value within each region was then measured. The range of the mean gray value was between 0 and 255, with 0 indicating the absence of reticulin fibers in the selected region and 255 indicating that the selected region was completely filled with reticulin fibers. After measurements, reticulin fiber densities among the cases were compared using the Mann-Whitney *U* test. Statistical analyses were performed using R Statistical Software (version 4.0.1). Results were considered to be significant when $P < 0.05$.

RESULTS

Differences in LVSEM images of the normal liver that were dependent on sample thicknesses

We initially investigated optimal sample thicknesses for the LVSEM imaging of Pt-Blue-stained and silver-impregnated specimens. We prepared 5-, 10-, and 20-μm-thick sections of a normal liver (Case No. 1). In Pt-Blue stained slides, thicker sections provided deeper three-dimensional images, but caused the more severe shrinkage or cracking of hepatocytes during LVSEM observations (Figs. 1A–C). Therefore, we selected 5-μm-thick sections for Pt-Blue staining. Similarly, in silver-impregnated sections, we observed deeper three-dimensional structures in thicker sections (Figs. 1D–F). However, since a focal deformation of hepatocyte plates was observed in 20-μm-thick sections (data not shown), which may have been an artifact that occurred during the cutting procedure, we selected 10-μm-thick sections for silver impregnation.

LM and LVSEM images of the normal liver

We assessed LM and LVSEM images of the normal liver using another liver specimen (Case No. 2). Under LM, the normal structure of hepatocyte plates and reticulin frameworks were clearly visualized by HE staining (Fig. 2A) and silver impregnation (Fig. 2B), respectively.

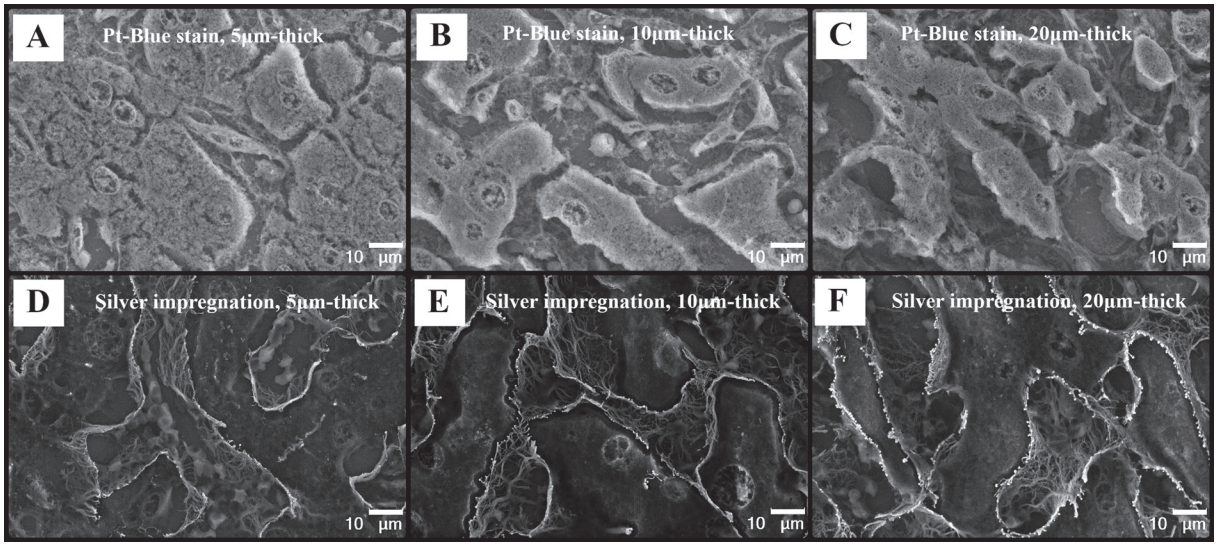

Fig. 1. LVSEM images of sections of a normal liver (Case No. 1) of different thicknesses with Pt-Blue staining (**A–C**) and silver impregnation (**D–F**). Thicknesses of 5 μm (**A, D**), 10 μm (**B, E**), and 20 μm (**C, F**). In both staining methods, thicker sections provided deeper three-dimensional images. However, in Pt-Blue-stained specimens, there were more shrunken or cracked hepatocytes in thicker sections. Observation signal: BSE + SE.

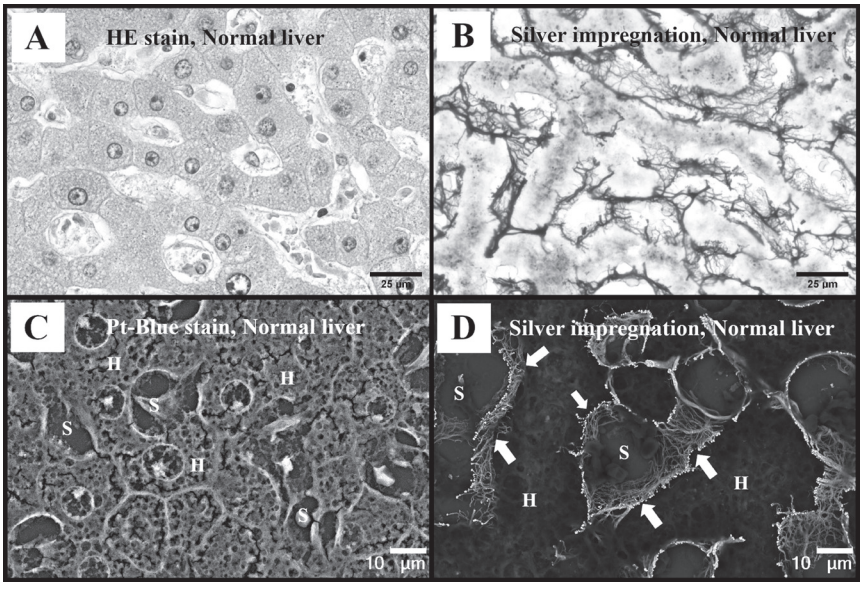

Fig. 2. Images of sections of a normal control liver (Case No. 2). HE-stained (**A**) and silver-impregnated (**B**) sections observed by LM. Pt-Blue-stained (**C**) and silver-impregnated (**D**) sections observed by LVSEM. Note that reticulin fibers running dendritically and wrapping around sinusoids from their outside are clearly observed in the LVSEM image of the silver-impregnated section (**D**, arrows). H, hepatocyte; S, sinusoid. Observation signal: BSE + SE (**C**) and BSE (**D**).

In LVSEM images of Pt-Blue-stained specimens, the structure of hepatic lobules was also clearly visualized, similar to that in LM images; however, its detailed ultrastructure was not discernible because of insufficient contrast and cracking artifacts (Fig. 2C). In LVSEM images of silver-impregnated specimens, reticulin fibers were clearly observed at a high brightness, running dendritically and wrapping around sinusoids from the outside three-dimensionally (Fig. 2D).

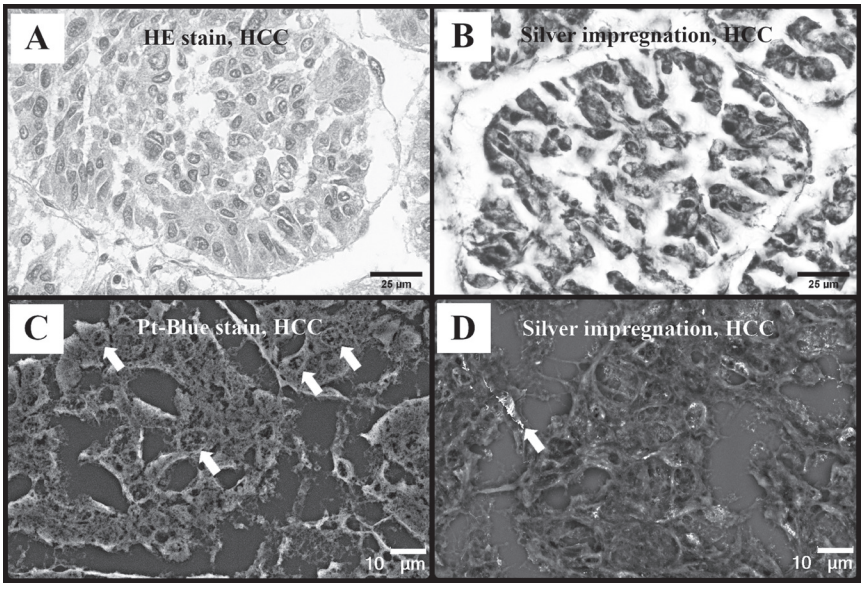

Fig. 3. Images of moderately to well-differentiated HCC (Case No. 4). HE-stained (**A**) and silver-impregnated (**B**) sections observed by LM. Pt-Blue-stained (**C**) and silver-impregnated (**D**) sections observed by LVSEM. Reticulin structures are obscure in the LM image of the silver-impregnated section (**B**). Tumor cells showing anisonucleosis are observed in the LVSEM image of the Pt-Blue section (**C**, arrows). In the LVSEM image of the silver-impregnated section, we observed the loss of the reticulin structure and fragments of reticulin fibers (**D**, arrow). Observation signal: BSE + SE (**C**) and BSE (**D**).

LM and LVSEM images of HCC and regenerative nodules/areas

The histologies of the two cases of HCC (Case Nos. 3 and 4) were similar to each other. In HE-stained sections, both tumors were mainly composed of medium to large trabeculae (Fig. 3A), focally showing a solid growth pattern and necrosis in Case No. 4. In LM observations of silver-impregnated specimens, the reticulin structure was obscured within HCC lesions (Fig. 3B). In LVSEM images of Pt-Blue-stained specimens, tumor cells were recognized by the presence of anisonucleosis; however, their detailed ultrastructure was not clear due to the shrinkage artifact (Fig. 3C). In LVSEM images of silver-impregnated specimens, the loss of the reticulin structure was recognized more clearly than when observed by LM, and even small fragments of reticulin fibers were detected in LVSEM observations (Fig. 3D).

In both cases of HCC, regenerative changes were noted in the background liver parenchyma. Specifically, Case No. 3 had regenerative nodules due to coexisting liver cirrhosis, whereas Case No. 4 had regenerative areas due to coexisting cholestasis and congestion. Under LM, these lesions were observed as cords of benign-looking hepatocytes in HE-stained specimens (Fig. 4A), and showed increased reticulin fibers in silver-impregnated specimens (Fig. 4B). Benign-looking hepatocytes lining up in cords were also observed in LVSEM images of Pt-Blue-stained specimens (Fig. 4C), which was similar to LM observations of HE-stained specimens. In LVSEM images of silver-impregnated specimens (Fig. 4D), the increase in reticulin fibers was recognized more clearly than when observed by LM.

Applicability of LVSEM imaging to a quantitative analysis

To assess the applicability of LVSEM imaging to a quantitative morphometric analysis, we performed the quantification of reticulin fiber density in the normal liver and regenerative nodules/areas (see Materials and Methods). Areas of HCC were excluded from the analysis because the reticulin structure had been completely destroyed within these areas. Due to the higher brightness of reticulin fibers than background objects (e.g. hepatocytes), we were able to properly extract the area of reticulin fibers while minimizing noise by thresholding the gray value (Figs. 5A–D). Using these binary images, we quantified reticulin fiber density in the sinusoidal wall. The results obtained showed that reticulin fiber density was significantly higher in regenerative areas/nodules (Case Nos. 3 and 4) than in the normal liver (Case Nos. 1 and 2) (Fig. 5E; $P < 0.05$). On the other hand, no significant differences were observed in reticulin fiber

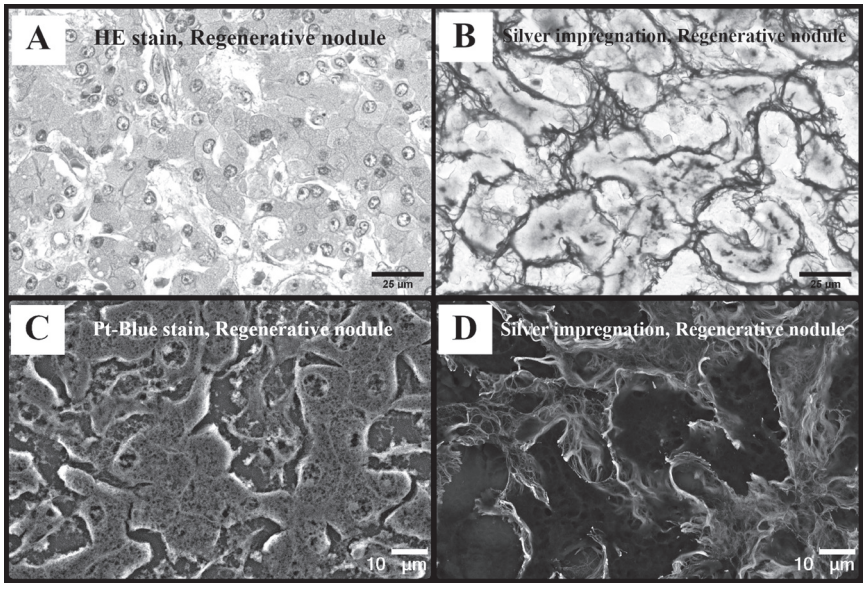

Fig. 4. Images of a part of a regenerative nodule in the background liver of HCC (Case No. 3). HE-stained (**A**) and silver-impregnated (**B**) sections observed by LM. Pt-Blue-stained (**C**) and silver-impregnated (**D**) sections observed by LVSEM. In the silver-impregnated specimen, an increase in reticulin fibers was clearly observed under LM (**B**), which was more pronounced under LVSEM (**D**). Observation signal: BSE + SE (**C**) and BSE (**D**).

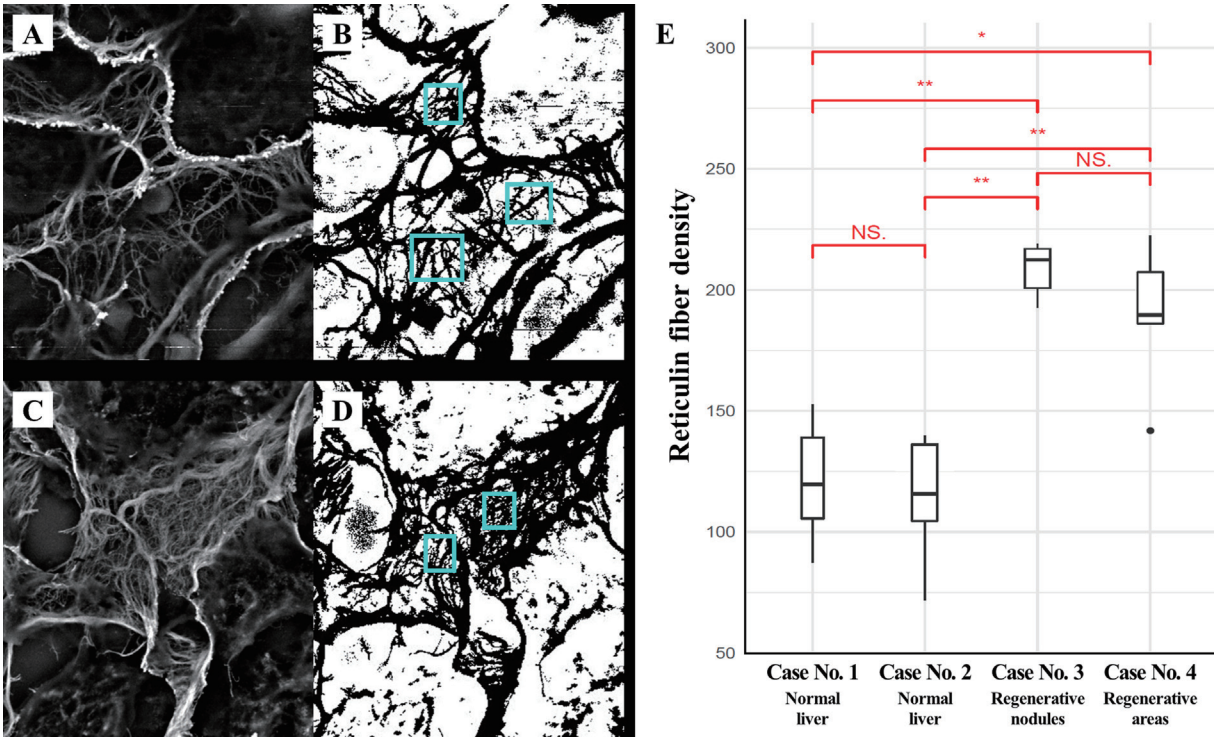

Fig. 5. Representative images showing the procedure of quantification of reticulin fiber density (**A**–**D**). An LVSEM image of a silver-impregnated sample of a normal liver (**A**; Case No. 2) was converted to a binary image displaying only areas of reticulin fibers (**B**). Similarly, an LVSEM image of a silver-impregnated sample with regenerative areas (**C**; Case No. 4) was converted to a binary image displaying only areas of reticulin fibers (**D**). The light blue rectangles in **B** and **D** indicate the selected regions for the quantification of reticulin fiber density. Note that at least 5 regions per image were selected for quantification (not all are shown here). Reticulin fiber density was significantly higher in regenerative nodules/areas (Case Nos. 3 and 4) than in the normal liver (Case Nos. 1 and 2), as shown in the box-and-whisker plot (**E**). $*P < 0.05$; $**P < 0.01$; N.S., not significant.

density between the regenerative nodules in Case No. 3 and the regenerative areas in Case No. 4. Similarly, reticulin fiber density was not significantly different between two normal liver tissues (Case Nos. 1 and 2).

DISCUSSION

The optimal sample thickness for LVSEM observations was investigated in the present study. This was because SEM is an excellent imaging modality for examining three-dimensional structures and, thus, we considered thicker sections were more suitable for LVSEM. As expected, thicker sections provided deeper three-dimensional images, but resulted in the more severe shrinkage or cracking of hepatocytes during observations of Pt-Blue-stained samples. The application of critical point drying[12] or t-butyl alcohol freeze drying[13] prior to LVSEM observations may prevent these artifacts; however, these procedures were not performed in the present study. On the other hand, no significant shrinking or cracking was noted in silver-impregnated samples regardless of the sample thickness, which may have been because silver impregnation hardened the samples. However, we detected focal deformation artifacts in 20-μm-thick silver-impregnated sections, which may have occurred during the cutting procedure. Therefore, we concluded that even in the silver impregnation method, sections with a thickness of 20 μm or more were suboptimal for LVSEM observations.

After selecting the optimal sample thickness, we successfully demonstrated the usefulness of LVSEM combined with Watanabe's silver impregnation for the three-dimensional imaging of reticulin structures in the liver. Specifically, we observed detailed reticulin fiber frameworks spreading dendritically and wrapping around sinusoids in the normal liver, and a marked increase in reticulin fibers in regenerative nodules/areas. We also noted that reticulin fiber frameworks were lost in areas of HCC, leaving only a few fragments of reticulin fibers. The utility of LVSEM combined with other silver staining techniques (such as the periodic acid methenamine silver stain) has been demonstrated in other organs, such as the kidney[7]; however, similar studies on the liver have been limited. To the best of our knowledge, the present study is the first to apply the combination of LVSEM and Watanabe's silver impregnation to observations of normal and diseased liver tissues. Since this technique is simple and applicable to widely available formalin-fixed archival tissues, it may be employed in a wide range of studies on liver diseases.

The present study also showed that LVSEM combined with silver impregnation may be applied to a quantitative analysis of reticulin fibers. Due to the higher brightness of reticulin fibers than background objects, we easily extracted the area of reticulin fibers and quantified it in a digital image analysis. This was possible because the BSE intensity in SEM is proportional to the average atomic number in the object. In silver-impregnated samples, reticulin fibers (and other argyrophilic materials) are selectively decorated by metallic silver, whereas other objects remain as organic matter with a smaller average atomic number. Therefore, the BSE intensity is stronger in areas of reticulin fibers than in other areas. Based on this principle, we successfully quantified reticulin fiber density and showed that it was significantly higher in regenerative nodules/areas than in the normal liver.

Few studies have quantified reticulin fibers in liver diseases, which may be because research on liver fibrosis has mainly focused on collagen fibers that markedly increase in various chronic liver diseases.[5] Previous studies that quantified reticulin fibers in liver fibrosis include an animal experimental study by Wen et al.[2] in which thioacetamide (TAA) and bile duct ligation (BDL) were utilized to induce liver fibrosis in rats. Changes in the amount of reticulin fibers over time were evaluated using a quantitative method under LM. The findings obtained demonstrated that the area of reticulin fibers along hepatic cords continuously decreased in both the TAA and BDL groups, and remained at a low level even after TAA was withdrawn for one month in the TAA group. This finding is in contrast to the present result showing that the amount of reticulin fibers was significantly higher in regenerative nodules/areas than in the normal liver. Although it is difficult to explain this discrepancy, it suggests that this experimental animal model does not necessarily reproduce the progression of liver fibrosis accurately in humans. Regarding neoplastic diseases, Vertemati et al.[14] performed a morphometric analysis using multiple parameters on nodular lesions in HCV-cirrhotic livers. They reported that surface fractions occupied by reticulin fibers were significantly smaller in HCC than in regenerative nodules and dysplastic nodules. However, since the loss of or a decrease in reticulin fibers in areas of HCC is already well known,[4] the precise quantification of reticulin fibers in neoplastic liver diseases may not provide further insights.

To the best of our knowledge, the present study is the first to investigate HCC using LVSEM. To date, many studies have investigated HCC using transmission electron microscopy; however, studies that examined these lesions using SEM were limited.[15, 16] This may be because SEM cannot visualize intracellular structures in detail. In the present study, we observed anisonucleosis

in the tumor areas of Pt-Blue-stained specimens, showing that the diagnosis of HCC is possible using LVSEM; however, we did not obtain any novel findings beyond those observed by conventional LM.

The limitations of the present study include the small number of samples examined. We only investigated four autopsy cases and did not perform the same assessment on biopsy samples because the main purpose of the present study was to develop a novel method to visualize the three-dimensional structures of the liver in detail using a simple procedure with LVSEM, which we considered to have been achieved even with this small sample size. The method presented herein needs to be applied to future studies with various purposes, including the more accurate diagnosis, classification, and risk stratification of patients with liver diseases, which will validate its clinical utility.

We are aware that the method of reticulin fiber quantification presented herein may not necessarily be appropriate for an accurate assessment of liver fibrosis. In the present study, we quantified reticulin fibers in only small areas of sinusoidal walls that were arbitrarily selected in one high-magnification image, and these small areas may not correctly represent the pathological status of the entire liver. However, it is important to note that quantification over a wider area does not necessarily result in a more accurate assessment of liver fibrosis. This is because the standard liver biopsy procedure yields only a very small portion of the entire liver and the potential for sampling errors is essentially unavoidable.[17] In addition, although several serum markers and non-invasive techniques, such as elastography, are utilized to evaluate liver fibrosis in current clinical practice, liver biopsy remains the gold standard despite its many limitations including complications, sampling errors, and intra- and interobserver variability.[17] In this sense, an optimal test method to accurately assess the liver fibrosis has not yet been fully established, and, thus, it can be said that any new method for the assessment of liver fibrosis deserves investigation for its clinical utility. Since the imaging method using LVSEM presented herein provides higher resolution images than conventional LM observations of silver-impregnated specimens, it is expected to enable the more sensitive detection of subtle changes in the amount and patterns of reticulin fibers that may be of clinical significance. However, the main purpose of the present study was to present a novel high-resolution imaging method of the liver with applicability to a quantitative analysis, not to provide a novel quantitative method itself to accurately assess liver fibrosis. Specific methods to assess changes in reticulin fibers that are of clinical significance are beyond the scope of this study and need to be investigated in future studies.

After optimization according to each purpose, a quantitative analysis of reticulin fibers using LVSEM is potentially applicable to the diagnosis of and research on various liver diseases. This technique may be used for the more detailed staging, risk stratification, and evaluation of the effects of therapeutic interventions in patients with chronic liver diseases, such as viral hepatitis and nonalcoholic steatohepatitis. Furthermore, it may be used in studies investigating subtle differences in reticulin fiber patterns among different etiologies of chronic liver diseases. If there are significant differences in reticulin fiber patterns among different etiologies, these findings may be useful for diagnosing the causes of liver diseases. Moreover, this technique may provide novel findings for the diagnosis of some space-occupying lesions of the liver. For example, some well-differentiated HCC have been shown to have a preserved reticulin fiber network[18]; therefore, these lesions may be difficult to correctly differentiate from benign and premalignant lesions, such as hepatocellular adenomas and dysplastic nodules, particularly in small biopsy specimens. However, since LVSEM enables the higher resolution imaging of reticulin fiber networks, it may be applied to studies investigating subtle differences in the amount and patterns of reticulin fibers among these lesions, which may contribute to a more accurate diagnosis using small samples.

In summary, we demonstrated the utility of LVSEM combined with Watanabe's silver impregnation for the detailed three-dimensional imaging of reticulin fibers in normal and diseased liver tissues. We also showed that this method is applicable to a digital image analysis for the quantification of reticulin fibers. The results obtained herein may be applied to future studies involving quantitative and qualitative evaluations of reticulin structures in various liver diseases.

Acknowledgments: The authors thank Medical English Service, Kyoto, Japan for proofreading the manuscript.

The authors declare no conflict of interest.

REFERENCES

1 Ushiki T. Collagen fibers, reticular fibers and elastic fibers. A comprehensive understanding from a morphological viewpoint. Arch Histol Cytol. 2002;65:109-26. DOI: 10.1679/aohc.65.109, PMID: 12164335

2 Wen SL, Feng S, Tang SH, Gao JH, Zhang L, Tong H, et al. Collapsed reticular network and its possible mechanism during the initiation and/or progression of hepatic fibrosis. Sci Rep. 2016;6:35426. DOI: 10.1038/srep35426, PMID: 27739503

3 Krishna M. Role of special stains in diagnostic liver pathology. Clin Liver Dis (Hoboken). 2013;2(suppl 1):S8-10. DOI: 10.1002/cld.148, PMID: 30992876
4 Torbenson M, Zen Y, Yeh MM. Hepatocellular carcinoma. In: AFIP atlas of tumor pathology, series 4. fascicle 27; tumors of the liver. Washington (DC): American Registry of Pathology; 2018. p. 39–96.
5 Arjmand A, Tsipouras MG, Tzallas AT, Forlano R, Manousou P, Giannakeas N. Quantification of liver fibrosis—a comparative study. Appl Sci (Basel). 2020;10:447. DOI: 10.3390/app10020447
6 Yavuz BG, Pestana RC, Abugabal YI, Krishnan S, Chen J, Hassan MM, et al. Origin and role of hepatic myofibroblasts in hepatocellular carcinoma. Oncotarget. 2020;11:1186-201. DOI: 10.18632/oncotarget.27532, PMID: 32284794
7 Miyazaki H, Uozaki H, Tojo A, Hirashima S, Inaga S, Sakuma K, et al. Application of low-vacuum scanning electron microscopy for renal biopsy specimens. Pathol Res Pract. 2012;208:503-9. DOI: 10.1016/j.prp.2012.05.006, PMID: 22795691
8 Inaga S, Hirashima S, Tanaka K, Katsumoto T, Kameie T, Nakane H, et al. Low vacuum scanning electron microscopy for paraffin sections utilizing the differential stainability of cells and tissues with platinum blue. Arch Histol Cytol. 2009;72:101-6. DOI: 10.1679/aohc.72.101, PMID: 20009346
9 Tanaka K, Inaga S, Iino A. New techniques for observing hydrous biological materials by low vacuum scanning electron microscopy and their applications. In: Motta PM, editor. Recent advances in microscopy of cells, tissues and organs. Rome, Antonio Defilo Editore; 1997. p. 31–35.
10 Inaga S, Katsumoto T, Tanaka K, Kameie T, Nakane H, Naguro T. Platinum blue as an alternative to uranyl acetate for staining in transmission electron microscopy. Arch Histol Cytol. 2007;70:43-9. DOI: 10.1679/aohc.70.43, PMID: 17558143
11 Schneider CA, Rasband WS, Eliceiri KW. NIH Image to ImageJ: 25 years of image analysis. Nat Methods. 2012;9:671-5. DOI: 10.1038/nmeth.2089, PMID: 22930834
12 Tanaka K, Iino A. Critical point drying method using dry ice. Stain Technol. 1974;49:203-6. DOI: 10.3109/10520297409116978, PMID: 4602349
13 Inoué T, Osatake H. Drying method of biological specimens for scanning method microscopy: the t-butyl alcohol. Arch Histol Cytol. 1988;51:53-9. DOI: 10.1679/aohc.51.53, PMID: 3137948
14 Vertemati M, Moscheni C, Petrella D, Lamperti L, Cossa M, Gambacorta M, et al. Morphometric analysis of hepatocellular nodular lesions in HCV cirrhosis. Pathol Res Pract. 2012;208:240-4. DOI: 10.1016/j.prp.2012.02.007, PMID: 22429827
15 Ogawa H, Itoshima T, Ukida M, Ito T, Kiyotoshi S, Kitadai M, et al. Scanning electron microscopy of experimentally induced hepatocellular carcinoma. Scan Electron Microsc. 1984;(Pt 1):359-68. PMID: 6740236
16 Kita K, Itoshima T, Tsuji T. Observation of microvascular casts of human hepatocellular carcinoma by scanning electron microscopy. Gastroenterol Jpn. 1991;26:319-28. DOI: 10.1007/BF02781920, PMID: 1653745
17 Chowdhury AB, Mehta KJ. Liver biopsy for assessment of chronic liver diseases: a synopsis. Clin Exp Med. 2022. DOI: 10.1007/s10238-022-00799-z, PMID: 35192111
18 Hong H, Patonay B, Finley J. Unusual reticulin staining pattern in well-differentiated hepatocellular carcinoma. Diagn Pathol. 2011;6:15. DOI: 10.1186/1746-1596-6-15, PMID: 21338527